Capacity Analysis of Joint Transmission CoMP with Adaptive Modulation

Qimei Cui, *Senior Member, IEEE*, Hengguo Song, Hui Wang, Mikko Valkama, *Senior Member, IEEE*, and Alexis A. Dowhuszko

***Abstract*—Joint Transmission (JT) based Coordinated Multipoint (CoMP) systems achieve high performance gains by allowing full coordination among multiple cells, transforming unwanted inter-cell interference into useful signal power. In this paper, we present an analytical model to perform adaptive modulation for a typical JT CoMP system, consisting of three transmission points, under a target Bit Error Rate (BER) constraint. Probability density functions of the Signal-to-Interference plus Noise Ratio (SINR) are derived for different JT CoMP schemes and, based on them, closed form expressions for the Average Spectral Efficiency (ASE) are obtained when adopting continuous-rate adaptive modulation. The study of ASE is also extended for the case of discrete-rate modulations, where the performance comparison of different practical quantized modulation schemes is carried out.**

***Index Terms*—Joint Transmission, Coordinated Multipoint, continuous-rate adaptive modulation, discrete-rate adaptive modulation, Average Spectral Efficiency**

I. Introduction

Coordinated Multipoint (CoMP) transmission harnesses multi-cell interference [1] and improves the coverage performance of cell-edge users. Due to that, CoMP has been included as an enabling technology of Fourth Generation (4G) wireless communication standards, such as 3GPP LTE-Advanced. Furthermore, CoMP is expected to suit even better in Fifth Generation (5G) networks, whose novel architectures will facilitate substantially larger amounts of data that can be currently exchanged among 4G Transmission Points (TPs) [2]. Among the most appealing CoMP schemes, Joint Transmission (JT) strategy offers the highest performance gains because both data and control information are fully shared among the active set of coordinated TPs.

The performance of JT CoMP has been extensively studied in the literature. For example, the authors of [3] presented the outage probability of Joint Processing (JP) CoMP when Maximum Ratio Transmission (MRT) is used at the TPs. Similarly, the macro diversity gain of CoMP in dense cellular networks was investigated in [4] assuming that locations of TPs form a random network topology. The authors of [5] focused on the performance of CoMP when orthogonal beamforming is utilized. Finally, the authors of [6] investigated the impact that quantized (and delayed) Channel State Information (CSI) has on the average data rate that JT and Coordinated Beamforming (CBF) CoMP can achieve.

Qimei Cui and Hengguo Song are with Beijing University of Posts and Telecommunications, Beijing, China (e-mail: {cuiqimei, shg}@bupt.edu.cn). Hui Wang is with the Jiangxi Transportation Institute, Nanchang, China (e-mail: whuissss@gmail.com). Mikko Valkama is with Tampere University of Technology, Tampere, Finland (e-mail: mikko.e.valkama@tut.fi). Alexis A. Dowhuszko is with the Centre Tecnològic de les Telecomunicacions de Catalunya (CTTC), Barcelona, Spain (e-mail: alexis.dowhuszko@cttc.es)

Fixed modulation schemes are simple to implement but, unfortunately, the Spectral Efficiency (SE) that they provide is very low under time-varying channel conditions and fixed target Bit Error Rate (BER). Adaptive modulation schemes, on the other hand, can offer higher SE for the same target BER by adjusting the modulation format according to the quality that the wireless channel experiences in each transmission time instant. The Average Spectral Efficiency (ASE) of different adaptive modulation schemes was studied in [7] for Dynamic Point Selection (DPS) and Dynamic Point Blanking (DPB) CoMP. Similarly, the precoding degree of freedom for link adaptation in JT CoMP was investigated in [8]. However, to the best of our knowledge, no theoretical analysis has been carried out so far on the capacity of adaptive modulation in JT CoMP.

In this paper, we investigate the performance of both continuous- and discrete-rate adaptive modulation in JT CoMP systems. Based on the fact that a typical CoMP system consists of three TPs at most, three different JT CoMP schemes are defined according to the number of active TPs that transmit information simultaneously to the same destination. An analytical model is presented to design the adaptive modulation scheme, where the target BER is set *a priori* to guarantee the Quality of Service in each transmission time interval.

The main contributions of this paper can be summarized as follows: Firstly, the Probability Density Function (PDF) of the received Signal-to-Interference plus Noise Ratio (SINR) is derived for the three JT CoMP schemes under consideration. Note that all these schemes rely solely on overall Channel Quality Indicator (CQI) reports, which are fed back regularly by the mobile user over a low-rate feedback channel. Secondly, closed form expressions for the ASE are derived considering the use of continuous-rate adaptive modulation. Finally, the ASE formulas are extended to the discrete-rate adaptive modulation case, where performance comparison is done using practical quantized modulation schemes. Numerical simulations are used to validate the presented theoretical analysis. Based on these results, notable gains are observed when JT CoMP adopts an adaptive modulation scheme that is properly designed.

The remainder of this paper is organized as follows: Section II presents the system model and assumptions. Section III describes continuous- and discrete-rate adaptive modulations for JT CoMP, and derives the closed form expressions for the ASE in each situation. Section IV analyzes the obtained simulation results. Finally, conclusions are drawn in Section V.

II. System Model

In order to provide a balance between performance gain and implementation complexity, it has been suggested that the

number of TPs in a CoMP cooperative cluster should not be much larger than three [9]. Therefore, we assume a typical JT CoMP system consisting of three TPs with single-antenna elements. In this situation, the instantaneous SINR that a generic single-antenna mobile user experiences in reception when served by TP_i is given by

$$\gamma_i = \frac{S_i}{I_{\text{out}} + P_N} = \frac{\alpha_i |h_i|^2}{I_{\text{out}} + P_N} = \bar{\gamma}_i |h_i|^2 \quad i \in \{1,2,3\}, \quad (1)$$

where S_i denotes the received signal power from TP_i, I_{out} represents the co-channel interference power generated outside the CoMP cooperation set, and P_N is the power of the Additive White Gaussian Noise (AWGN). In case of rich scattering and short delay spread, instantaneous channel gain h_i from TP_i is described by a complex Gaussian random variable with zero mean and unit variance. Moreover, α_i represents a scaling parameter that combines the effect of mean transmission power, path loss attenuation, and shadowing. For the sake of simplicity, we assume that α_i remains constant during the whole duration of the communication (*i.e.*, mobile users do not change their locations and no fast power control mechanism is applied in transmission to compensate fast fading). The CQI is first estimated in downlink by the mobile user and is then reported back to the serving TPs to select a common modulation format that guarantees the target BER. In order to keep feedback overhead low, no CSI on individual wireless links is reported to the TPs separately. Based on this limitation, only the Non-Coherent alternative of JT CoMP is considered in this paper.

Let us assume a CoMP scenario with three TPs, namely TP_i, TP_j, and TP_k, respectively. Then, three different JT CoMP types can be configured according to the number of active TPs in the cooperation set, with SINR (or equivalently CQI) formulas attaining the forms that are detailed below.

- **Type I**: The three TPs transmit data jointly. Then, the corresponding SINR is given by
$$q_1 = \frac{S_i + S_j + S_k}{I_{\text{out}} + P_N} = \gamma_i + \gamma_j + \gamma_k \quad i,j,k \in \{1,2,3\} \text{ with } i \neq j \neq k. \quad (2)$$
- **Type II**: Two TPs transmit data together (*i.e.*, TP_i and TP_j), whereas the signal from the third TP (*i.e.*, TP_k) is regarded as interference. The SINR in this situation is
$$q_2 = \frac{S_i + S_j}{S_k + I_{\text{out}} + P_N} = \frac{\gamma_i + \gamma_j}{\gamma_k + 1} \quad i,j,k \in \{1,2,3\} \text{ with } i \neq j \neq k. \quad (3)$$
- **Type III**: Only one TP transmits useful information (*i.e.*, TP_i), while the other two TPs (*i.e.*, TP_j and TP_k) serve a different mobile user generating co-channel interference. This is the baseline non-CoMP transmission case, where the SINR expression attains the form
$$q_3 = \frac{S_i}{S_j + S_k + P_N + I_{\text{out}}} = \frac{\gamma_i}{\gamma_j + \gamma_k + 1} \quad i,j,k \in \{1,2,3\} \text{ with } i \neq j \neq k. \quad (4)$$

M-ary Quadrature Amplitude Modulation (M-QAM) schemes are widely used when designing adaptive modulation methods. For example, 3GPP LTE-Advanced adopts QPSK, 16-QAM, 64-QAM, and 256-QAM for the downlink physical shared channel. Therefore, we focus on link adaptation methods that rely on M-QAM formats and, for simplicity, we make symbol duration equal to the inverse of the channel bandwidth. Moreover, we assume that instantaneous BER of a given M-QAM format can be accurately approximated [1] by

$$\text{BER} \approx c_1 e^{-\frac{c_2 \gamma}{2^{\eta}-1}}, \quad (5)$$

where $c_1 = 0.2$ and $c_2 = 1.5$, whereas η and γ denote the SE and SINR, respectively [10, 11]. With the aid of (5), we will study the ASE that JT CoMP provides under a BER constraint.

III. Continuous- and Discrete-Rate Adaptation

A. Capacity Analysis for Continuous-rate Adaptation Joint Transmission CoMP

In this section we assume that perfect CQI and a large number of modulation formats are available at the TPs. Therefore, actual instantaneous BER becomes equal to BER_{tar}, which is the target value of the BER in each transmission time interval. Then, according to the corresponding CQI definition, the number of transmitted bits per symbol can be derived from (5) as follows:

$$\eta = \log_2(c\gamma + 1), \quad (6)$$

where $c = c_2 / \ln(c_1/\text{BER}_{\text{tar}})$. Thus, the ASE is given by

$$\eta_{\text{ave}} = \mathbb{E}_{\gamma}\{\eta\} = \int_0^{\infty} \eta(\gamma)\, f_q(\gamma)\, d\gamma, \quad (7)$$

where $f_q(\gamma)$ is the PDF of CQI q, which depends on the definition of SINR that is used for each JT CoMP type.

Lemma: The PDFs of q_1, q_2 and q_3 can be written as:

$$f_{q_1}(x\,|\bar{\gamma}_i, \bar{\gamma}_j, \bar{\gamma}_k) = \begin{cases} \bar{\gamma}_i \dfrac{e^{-\frac{x}{\bar{\gamma}_i}} - e^{-\frac{x}{\bar{\gamma}}}}{(\bar{\gamma}_i - \bar{\gamma})^2} + \dfrac{x e^{-\frac{x}{\bar{\gamma}}}}{\bar{\gamma}(\bar{\gamma} - \bar{\gamma}_i)} & \text{for } \bar{\gamma}_j = \bar{\gamma}_k = \bar{\gamma}, \\ \bar{\gamma}_j \dfrac{e^{-\frac{x}{\bar{\gamma}_i}} - e^{-\frac{x}{\bar{\gamma}_j}}}{(\bar{\gamma}_i - \bar{\gamma}_j)(\bar{\gamma}_j - \bar{\gamma}_k)} - \bar{\gamma}_k \dfrac{e^{-\frac{x}{\bar{\gamma}_i}} - e^{-\frac{x}{\bar{\gamma}_k}}}{(\bar{\gamma}_j - \bar{\gamma}_k)(\bar{\gamma}_i - \bar{\gamma}_k)} & \text{for } \bar{\gamma}_j \neq \bar{\gamma}_k, \end{cases} \quad (8)$$

$$f_{q_2}(x\,|\bar{\gamma}_i, \bar{\gamma}_j, \bar{\gamma}_k) = \begin{cases} \mathrm{e}^{\frac{x}{\bar{\gamma}}} x \left[\dfrac{1}{\bar{\gamma}(\bar{\gamma} + \bar{\gamma}_k x)} + \dfrac{2\bar{\gamma}_k}{(\bar{\gamma} + \bar{\gamma}_k x)^2} + \dfrac{2\bar{\gamma}\bar{\gamma}_k^2}{(\bar{\gamma} + \bar{\gamma}_k x)^3} \right] & \text{for } \bar{\gamma}_i = \bar{\gamma}_j = \bar{\gamma}, \\ \dfrac{\bar{\gamma}_i e^{-\frac{x}{\bar{\gamma}_i}} (\bar{\gamma}_i + \bar{\gamma}_i\bar{\gamma}_k + \bar{\gamma}_k x)}{(\bar{\gamma}_i + \bar{\gamma}_k x)^2 (\bar{\gamma}_i - \bar{\gamma}_j)} - \dfrac{\bar{\gamma}_j e^{-\frac{x}{\bar{\gamma}_j}} (\bar{\gamma}_j + \bar{\gamma}_j\bar{\gamma}_k + \bar{\gamma}_k x)}{(\bar{\gamma}_j + \bar{\gamma}_k x)^2 (\bar{\gamma}_i - \bar{\gamma}_j)} & \text{for } \bar{\gamma}_i \neq \bar{\gamma}_j, \end{cases} \quad (9)$$

$$f_{q_3}(x\,|\bar{\gamma}_i, \bar{\gamma}_j, \bar{\gamma}_k) = \begin{cases} \left[\dfrac{2\bar{\gamma}\bar{\gamma}_i^2}{(\bar{\gamma}_i + \bar{\gamma} x)^3} + \dfrac{\bar{\gamma}_i}{(\bar{\gamma}_i + \bar{\gamma} x)^2} \right] e^{-\frac{x}{\bar{\gamma}_i}} & \text{for } \bar{\gamma}_j = \bar{\gamma}_k = \bar{\gamma}, \\ \dfrac{e^{-\frac{x}{\bar{\gamma}_i}} \left[\frac{1}{\frac{x}{\bar{\gamma}_i} + \frac{1}{\bar{\gamma}_j}} - \frac{1}{\frac{x}{\bar{\gamma}_i} + \frac{1}{\bar{\gamma}_k}} + \frac{1}{\left(\frac{x}{\bar{\gamma}_i} + \frac{1}{\bar{\gamma}_j}\right)^2} - \frac{1}{\left(\frac{x}{\bar{\gamma}_i} + \frac{1}{\bar{\gamma}_k}\right)^2} \right]}{\bar{\gamma}_i (\bar{\gamma}_j - \bar{\gamma}_k)} & \text{for } \bar{\gamma}_j \neq \bar{\gamma}_k. \end{cases} \quad (10)$$

[1] This approximation is tight within 1 dB for $M \geq 4$ and $\text{BER} \leq 10^3$.

Proof: See Appendix A.

Theorem: For the three JT CoMP types under consideration, the ASE that the scheduled mobile user experiences in downlink is given by the following closed form expressions:

$$\eta_{\text{ave},1} = \begin{cases} \dfrac{\left(\bar{\gamma} - c\bar{\gamma}^2 - \bar{\gamma}_i + 2\,c\,\bar{\gamma}\,\bar{\gamma}_i\right) \mathrm{e}^{\frac{1}{c\bar{\gamma}}}\,\mathrm{Ei}\left(-\frac{1}{c\bar{\gamma}}\right)}{c\left(\bar{\gamma}_i - \bar{\gamma}\right)^2 \ln 2} \\ \quad - \dfrac{\bar{\gamma}_i^2 \mathrm{e}^{\frac{1}{c\,\bar{\gamma}_i}}\,\mathrm{Ei}\left(-\frac{1}{c\bar{\gamma}_i}\right)}{\left(\bar{\gamma}_i - \bar{\gamma}\right)^2 \ln 2} - \dfrac{\bar{\gamma}}{\left(\bar{\gamma}_i - \bar{\gamma}\right) \ln 2} & \bar{\gamma}_j = \bar{\gamma}_k = \bar{\gamma}, \\ \dfrac{\bar{\gamma}_j^2\,\mathrm{e}^{\frac{1}{c\bar{\gamma}_j}}\,\mathrm{Ei}\left(-\frac{1}{c\bar{\gamma}_j}\right)}{(\bar{\gamma}_i - \bar{\gamma}_j)(\bar{\gamma}_j - \bar{\gamma}_k)\ln 2} - \dfrac{\bar{\gamma}_i^2\,\mathrm{e}^{\frac{1}{c\bar{\gamma}_i}}\,\mathrm{Ei}\left(-\frac{1}{c\bar{\gamma}_i}\right)}{(\bar{\gamma}_i - \bar{\gamma}_j)(\bar{\gamma}_i - \bar{\gamma}_k)\ln 2} \\ \quad - \dfrac{\bar{\gamma}_k^2\,\mathrm{e}^{\frac{1}{c\bar{\gamma}_k}}\,\mathrm{Ei}\left(-\frac{1}{c\bar{\gamma}_k}\right)}{(\bar{\gamma}_i - \bar{\gamma}_k)(\bar{\gamma}_j - \bar{\gamma}_k)\ln 2} & \bar{\gamma}_j \neq \bar{\gamma}_k, \end{cases} \tag{11}$$

$$\eta_{\text{ave},2} = \begin{cases} \dfrac{c\,\bar{\gamma}\,\mathrm{e}^{\frac{1}{\bar{\gamma}_k}}\,\mathrm{Ei}\left(-\frac{1}{\bar{\gamma}_k}\right)}{(c\bar{\gamma} - \bar{\gamma}_k)\ln 2}\left[1 - \dfrac{\bar{\gamma}_k}{c\bar{\gamma} - \bar{\gamma}_k}\right] + \dfrac{c\bar{\gamma}}{(c\bar{\gamma} - \bar{\gamma}_k)\ln 2} \\ \quad - \dfrac{\mathrm{e}^{\frac{1}{c\bar{\gamma}}}\mathrm{Ei}\left(-\frac{1}{c\bar{\gamma}}\right)}{(c\bar{\gamma} - \bar{\gamma}_k)\ln 2}\left[c\bar{\gamma} - 1 - \dfrac{c\,\bar{\gamma}\,\bar{\gamma}_k}{c\bar{\gamma} - \bar{\gamma}_k}\right] & \bar{\gamma}_i = \bar{\gamma}_j = \bar{\gamma}, \\ \dfrac{c\,\bar{\gamma}_j^2\,e^{\frac{1}{c\bar{\gamma}_j}}\,\mathrm{Ei}\left(-\frac{1}{c\bar{\gamma}_j}\right)}{(\bar{\gamma}_i - \bar{\gamma}_j)\,(c\bar{\gamma}_j - \bar{\gamma}_k)\ln 2} - \dfrac{c\bar{\gamma}_i^2 e^{\frac{1}{c\bar{\gamma}_i}}\,\mathrm{Ei}\left(-\frac{1}{c\bar{\gamma}_i}\right)}{(\bar{\gamma}_i - \bar{\gamma}_j)\,(c\bar{\gamma}_i - \bar{\gamma}_k)\ln 2} \\ \quad + \dfrac{c\,\mathrm{e}^{\frac{1}{\bar{\gamma}_k}}\,(c\,\bar{\gamma}_i\,\bar{\gamma}_j - \bar{\gamma}_i\,\bar{\gamma}_k - \bar{\gamma}_j\bar{\gamma}_k)\,\mathrm{Ei}\left(-\frac{1}{\bar{\gamma}_k}\right)}{(c\,\bar{\gamma}_j - \bar{\gamma}_k)\,(c\,\bar{\gamma}_i - \bar{\gamma}_k)\ln 2} & \bar{\gamma}_i \neq \bar{\gamma}_j, \end{cases} \tag{12}$$

$$\eta_{\text{ave},3} = \begin{cases} \dfrac{c\bar{\gamma}_i}{\bar{\gamma}(\bar{\gamma} - c\bar{\gamma}_i)^2 \ln 2}\left[(\bar{\gamma} - c\bar{\gamma}_i + c\bar{\gamma}\bar{\gamma}_i)e^{\frac{1}{\bar{\gamma}}}\mathrm{Ei}\left(-\dfrac{1}{\bar{\gamma}}\right)\right. \\ \quad \left. + \bar{\gamma}\left(\bar{\gamma} - c\bar{\gamma}_i - c\bar{\gamma}_i e^{\frac{1}{c\bar{\gamma}_i}}\mathrm{Ei}\left(-\dfrac{1}{c\bar{\gamma}_i}\right)\right)\right] & \bar{\gamma}_j = \bar{\gamma}_k = \bar{\gamma}, \\ \dfrac{c\bar{\gamma}_i}{(\bar{\gamma}_j - \bar{\gamma}_k)\ln 2}\left[\dfrac{\bar{\gamma}_j\left(e^{\frac{1}{\bar{\gamma}_j}}\mathrm{Ei}\left(-\frac{1}{\bar{\gamma}_j}\right) - e^{\frac{1}{c\bar{\gamma}_i}}\mathrm{Ei}\left(-\frac{1}{\bar{\gamma}_i}\right)\right)}{c\bar{\gamma}_i - \bar{\gamma}_j}\right. \\ \quad \left. - \dfrac{\bar{\gamma}_k\left(e^{\frac{1}{\bar{\gamma}_k}}\mathrm{Ei}\left(-\frac{1}{\bar{\gamma}_k}\right) - e^{\frac{1}{c\bar{\gamma}_i}}\mathrm{Ei}\left(-\frac{1}{\bar{\gamma}_i}\right)\right)}{c\bar{\gamma}_i - \bar{\gamma}_k}\right] & \bar{\gamma}_j \neq \bar{\gamma}_k, \end{cases} \tag{13}$$

where $\mathrm{Ei}(t) = \int_{-\infty}^{t} x^{-1}e^{x}\,dx$ denotes the exponential integral function.

Proof: See Appendix B.

B. Capacity Analysis for Discrete-rate Adaptation Joint Transmission CoMP

For discrete-rate M-QAM, the constellation set is defined as $\{M_n = 2^n : n = 0, \ldots, N\}$, where N determines the maximum constellation size and M_0 means no data transmission. Then, the instantaneous SINR is divided into $N+1$ non-overlapping regions $\{[\rho_0, \rho_1); [\rho_1, \rho_2); \ldots; [\rho_N, \rho_{N+1})\}$, where $\{\rho_n : n = 1, \ldots, N\}$ are the switching thresholds. Note that in the previous definition, $\rho_0 = 0$ and $\rho_{N+1} = \infty$ for all modulation orders. The M-QAM scheme with constellation size M_n is selected for transmission if the instantaneous SINR falls into the n-th region, which is defined as $[\rho_n, \rho_{n+1})$. Consequently, the transmission rate is $b_n = \log_2(M_n)$ bits/symbol.

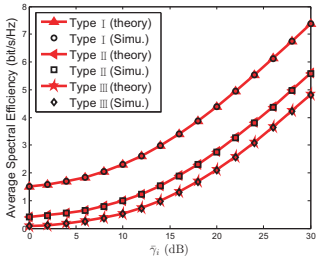

Fig. 1. Monte Carlo simulations for continuous-rate JT CoMP types ($\text{BER}_{\text{tar}} = 10^{-3}$, $\bar{\gamma}_j = 4.5$ dB, and $\bar{\gamma}_k = 5.5$ dB).

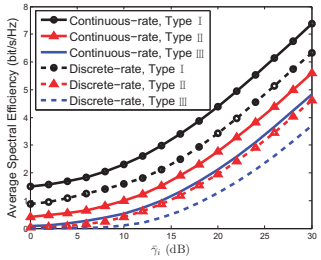

Fig. 2. ASE for JT CoMP with continuous- and discrete-rate adaptive modulations ($\text{BER}_{\text{tar}} = 10^{-3}$, $\bar{\gamma}_j = 4.5$ dB, and $\bar{\gamma}_k = 5.5$ dB).

By setting the BER in (5) equal to BER_{tar}, the switching thresholds $\{\rho_n\}$ can be expressed as the required SINRs to achieve the target BER as follows:

$$\rho_n = \begin{cases} 0 & n = 0, \\ \left[\text{erfc}^{-1}\left(\text{BER}_{\text{tar}}\right)\right]^2 & n = 1, \\ \left(M_n - 1\right)/A & n = 2, \ldots, N, \\ \infty & n = N+1, \end{cases} \tag{14}$$

where $\text{erfc}^{-1}(x)$ denotes the inverse complementary error function and $A = -1.5/\ln(\text{BER}_{\text{tar}})$. Since (5) is a tight BER approximation only for $M \geq 4$, the threshold ρ_1 can be selected using the exact BER formula for BPSK [12]. When the switching thresholds are determined with the approximated BER formulas for higher order constellations, the communication system will operate at a BER that is below the target BER_{tar}. For example, when $\text{BER}_{\text{tar}} = 10^{-3}$ and the modulation scheme is square M-QAM, the SINR switching thresholds are 6.79, 10.25, 17.24, 23.47, and 29.55 dB for BPSK (1 bit), QPSK (2 bits), 16-QAM (4 bits), 64-QAM (6 bits), and 256-QAM (8 bits), respectively.

Based on the previous analysis, the ASE for discrete-rate adaptation is given by

$$\eta_{\text{ave}} = \sum_{n=1}^{N} \log_2(M_n) \int_{\rho_n}^{\rho_{n+1}} f_q(\gamma)\,d\gamma. \tag{15}$$

Closed-form expressions for ASE can be obtained from (15) when discrete-rate adaptation is used with different JT CoMP types. As expected, these formulas vary as the quantized modulation schemes change. Therefore, no direct closed form expressions are given here. Nevertheless, the simulated performance results that quantized modulation schemes provide are compared in the following section.

IV. Numerical Results

In this section we study the ASE that JT CoMP provides to the scheduled mobile user in different scenarios. For the continuous-rate adaptation JT CoMP, the ASE is calculated using (11)–(13). For the discrete-rate adaptation case, on the other hand, the ASE is obtained using (15). From Fig. 1, it is possible to confirm that the results obtained with the aid of Monte Carlo simulations coincide with the theoretical ones, validating the analysis that has been proposed in Section III.

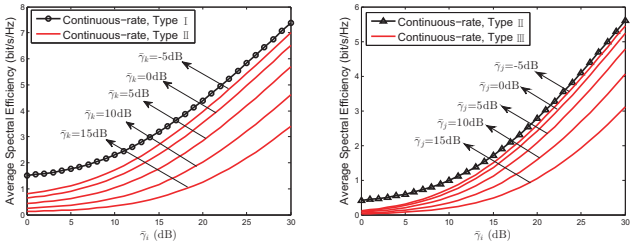

(a) (b)

Fig. 3. Average spectral efficiency for JT CoMP with continuous-rate adaptive modulation and different $\overline{\gamma}_j$ and $\overline{\gamma}_k$. Unless otherwise stateted, $\overline{\gamma}_j = 4.5\,\text{dB}$ and $\overline{\gamma}_k = 5.5\,\text{dB}$.

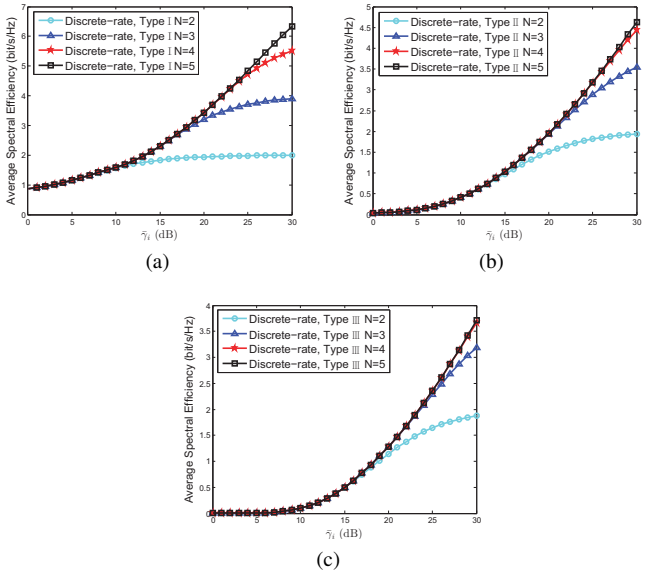

(a) (b)

(c)

Fig. 4. Average spectral efficiency for JT CoMP with discrete-rate adaptation with different quantized modulation schemes ($\text{BER}_{\text{tar}} = 10^{-3}$, $\overline{\gamma}_j = 4.5\,\text{dB}$, and $\overline{\gamma}_k = 5.5\,\text{dB}$).

The ASE values that are feasible with continuous-rate adaptive modulation are shown in Fig. 1 when $\text{BER}_{\text{tar}} = 10^{-3}$, $\overline{\gamma}_j = 4.5\,\text{dB}$, and $\overline{\gamma}_k = 5.5\,\text{dB}$. As expected, Type I gives the best performance whereas Type III gives the worst. For example, when $\overline{\gamma}_i = 20\,\text{dB}$, the ASE is $2.1141\,\text{bps/Hz}$ for Type III and $4.3943\,\text{bps/Hz}$ for Type I. Figure 2 compares the performance of continuous- and discrete-rate adaptive modulations and shows that, for each of the different JT CoMP types, continuous-rate adaptation performs better than the discrete-rate counterpart. It is worth noticing that $\text{BER} = 10^{-3}$ is obtained exactly for all fading states in continuous-rate adaptation, whereas in discrete-rate adaptation the performance is slightly better since $\text{BER} \leq 10^{-3}$ holds.

In Fig. 3, we evaluate the ASE of continuous-rate adaptive JT CoMP types I-III for different values of $\overline{\gamma}_j$ and $\overline{\gamma}_k$. From Fig. 3 (a) it is possible to observe that by decreasing $\overline{\gamma}_k$ (with $\overline{\gamma}_j = 4.5\,\text{dB}$), the performance of Type II approaches that of Type I (with $\overline{\gamma}_k = 5.5\,\text{dB}$). Similarly, it is possible to see from Fig. 3 (b) that by decreasing $\overline{\gamma}_j$ with fixed $\overline{\gamma}_k = 5.5\,\text{dB}$, the performance of Type III approaches that of Type II (with $\overline{\gamma}_j = 4.5\,\text{dB}$). Therefore, we can conclude that when signal strength from TPs is weak (*i.e.*, the system works in a noise-limited regime), it is better to increase the received signal power by increasing the number of TPs in the cooperative cluster (using either Type I or Type II), rather than decreasing the interference power that the co-located TPs generate when no cooperation is implemented (*i.e.*, JT CoMP Type III).

Figure 4 compares the performance of different quantized modulation schemes and JT CoMP types as function of $\overline{\gamma}_i$, when $\overline{\gamma}_j = 4.5\,\text{dB}$ and $\overline{\gamma}_k = 5.5\,\text{dB}$ are kept fixed. From this figure it is possible to observe that the constellation set that discrete-rate adaptation should support to experience a negligible ASE loss does not need to be the same for all JT CoMP types. Therefore, we can conclude that the appropriate quantized modulation scheme should be selected not only according to the JT CoMP type, but also to the mean received signal power that is experienced from each individual TP.

V. Conclusions

In this paper, we presented an analytical model to characterize the performance of continuous- and discrete-rate adaptive modulations when combined with JT CoMP. The PDFs for the instantaneous SINR were derived assuming three different JT CoMP types. With the aid of these density functions, and considering a target BER, closed form expressions for the ASE were obtained when continuous-rate adaptive modulation is adopted. The study was also extended to practical discrete-rate adaptive modulation case, where M-QAM constellations of different orders are used. Numerical simulations were used to validate the derived analytical results. It was observed that JT CoMP with adaptive modulation gives notable performance gains with respect to the baseline transmission method without cooperation. The derived results provide valuable insight and guidance for adopting and developing JT CoMP in contemporary 4G and future 5G networks.

Appendix A

Proof: Since $h_i, h_j, h_k \sim \mathcal{CN}(0,1)$, then $\gamma_i, \gamma_j, \gamma_k$ are exponentially distributed with $f_{\gamma_i}(x) = \frac{1}{\bar{\gamma}_i} e^{-\frac{x}{\bar{\gamma}_i}}$, $f_{\gamma_j}(x) = \frac{1}{\bar{\gamma}_j} e^{-\frac{x}{\bar{\gamma}_j}}$, and $f_{\gamma_k}(x) = \frac{1}{\bar{\gamma}_k} e^{-\frac{x}{\bar{\gamma}_k}}$, respectively [13]. For Type I we assume $v = \gamma_j + \gamma_k \geq 0$, whereas for Type II we consider $v = \gamma_i + \gamma_j \geq 0$. We further assume $v = \gamma_j + \gamma_k + 1 \geq 1$ for Type III. The derivations of (9) and (10) are similar to that of (8); hence, we focus on the latter. Let $v = \gamma_j + \gamma_k \geq 0$; then, after deriving the joint PDF of (q_1, v), the PDF of q_1 can be obtained as a marginal PDF. Therefore, we first derive the PDF of v by integrating the joint PDF of (γ_j, v) over γ_j.

Since γ_j and γ_k represent the instantaneous received SINRs from different TPs, their marginal PDFs can be considered independent and identically distributed. Due to that,

$$f_{(\gamma_j,\gamma_k)}(x,y) = f_{\gamma_j}(x)\, f_{\gamma_k}(y) = \frac{1}{\bar{\gamma}_j \bar{\gamma}_k} e^{-\frac{x}{\bar{\gamma}_j} - \frac{y}{\bar{\gamma}_k}}. \qquad (16)$$

By using the bivariate transformation theory, it is possible to show that the joint PDF of (γ_j, v) is given by

$$f_{(\gamma_j,v)}(x,z) = \begin{cases} \frac{1}{\bar{\gamma}_j \bar{\gamma}_k} e^{-\frac{x}{\bar{\gamma}_j} - \frac{(z-x)}{\bar{\gamma}_k}} & 0 \leq x \leq z, \\ 0 & \text{elsewhere.} \end{cases} \qquad (17)$$

Thus, $f_v(z)$ is the marginal distribution of $f_{(\gamma_j,v)}(x,z)$, which can be obtained by solving $f_v(z)=\int_{-\infty}^{+\infty} f_{(\gamma_j,v)}(x,z)\,dx$, *i.e.*,

$$f_v(z)=\begin{cases}\int_0^z \frac{1}{\bar{\gamma}^2}e^{-\frac{z}{\bar{\gamma}}}\,dx=\frac{1}{\bar{\gamma}^2}ze^{-\frac{z}{\bar{\gamma}}} & \bar{\gamma}_j=\bar{\gamma}_k=\bar{\gamma},\\ \int_0^z \frac{1}{\bar{\gamma}_j\bar{\gamma}_k}e^{-\frac{x}{\bar{\gamma}_j}-\frac{(z-x)}{\bar{\gamma}_k}}\,dx=\frac{e^{-\frac{z}{\bar{\gamma}_j}}-e^{-\frac{z}{\bar{\gamma}_k}}}{\bar{\gamma}_j-\bar{\gamma}_k} & \bar{\gamma}_j\neq\bar{\gamma}_k.\end{cases} \tag{18}$$

As γ_i, γ_j, and γ_k are independent random variables, the joint PDF of (γ_i, v) can be obtained as follows:

$$\begin{aligned}f_{(\gamma_i,v)}(t,z)&=f_{\gamma_i}(t)\,f_v(z)\\&=\begin{cases}\frac{1}{\bar{\gamma}_i}\frac{1}{\bar{\gamma}^2}ze^{-\frac{z}{\bar{\gamma}}}e^{-\frac{t}{\bar{\gamma}_i}} & \bar{\gamma}_j=\bar{\gamma}_k=\bar{\gamma},\\ \frac{e^{-\frac{t}{\bar{\gamma}_i}}(e^{-\frac{z}{\bar{\gamma}_j}}-e^{-\frac{z}{\bar{\gamma}_k}})}{\bar{\gamma}_i(\bar{\gamma}_j-\bar{\gamma}_k)} & \bar{\gamma}_j\neq\bar{\gamma}_k.\end{cases}\end{aligned} \tag{19}$$

Using again the bivariate transformation theory, the joint PDF of (q_1, v) can be expressed as

$$\begin{aligned}f_{(q_1,v)}(u,z)&=f_{(\gamma_i,v)}(u-z,z)\\&=\begin{cases}\frac{1}{\bar{\gamma}_i}\frac{1}{\bar{\gamma}^2}ze^{-\frac{z}{\bar{\gamma}}}e^{-\frac{u-z}{\bar{\gamma}_i}} & \bar{\gamma}_j=\bar{\gamma}_k=\bar{\gamma},\\ \frac{e^{-\frac{u-z}{\bar{\gamma}_i}}(e^{-\frac{z}{\bar{\gamma}_j}}-e^{-\frac{z}{\bar{\gamma}_k}})}{\bar{\gamma}_i(\bar{\gamma}_j-\bar{\gamma}_k)} & \bar{\gamma}_j\neq\bar{\gamma}_k.\end{cases}\end{aligned} \tag{20}$$

Finally, integrating the joint density function $f_{(q_1,v)}(u,z)$ with respect to z, closed form expression (8) is obtained.

APPENDIX B

Proof: Substituting (8) and (9) in (7), it is possible to derive (11) and (12). The key steps to reach (13) consist in substituting (10) in (7) and using integration by parts to simplify the terms to be integrated. When $\bar{\gamma}_j=\bar{\gamma}_k=\bar{\gamma}$,

$$\begin{aligned}\eta_{\text{ave},3}&=\int_0^\infty \log_2(cx+1)\left[\frac{2\bar{\gamma}\bar{\gamma}_i^2}{(\bar{\gamma}_i+\bar{\gamma}x)^3}+\frac{\bar{\gamma}_i}{(\bar{\gamma}_i+\bar{\gamma}x)^2}\right]e^{-\frac{x}{\bar{\gamma}_i}}\,dx\\&=\int_0^\infty \log_2(cx+1)\,\frac{\bar{\gamma}_i}{(\bar{\gamma}_i+\bar{\gamma}x)^2}e^{-\frac{x}{\bar{\gamma}_i}}\,dx\\&\quad+\int_0^\infty \log_2(cx+1)\,\frac{2\bar{\gamma}\bar{\gamma}_i^2}{(\bar{\gamma}_i+\bar{\gamma}x)^3}e^{-\frac{x}{\bar{\gamma}_i}}\,dx\end{aligned} \tag{21}$$

where the first term on the right hand side can be further expanded through integration by parts as

$$\begin{aligned}&\int_0^\infty \log_2(cx+1)\,\frac{\bar{\gamma}_i}{(\bar{\gamma}_i+\bar{\gamma}x)^2}e^{-\frac{x}{\bar{\gamma}_i}}\,dx \overset{\text{Integration by parts}}{=}\\&-\bar{\gamma}_i e^{-\frac{x}{\bar{\gamma}_i}}\log_2(cx+1)\,\frac{\bar{\gamma}_i}{(\bar{\gamma}_i+\bar{\gamma}x)^2}\Bigg|_0^\infty\\&+\int_0^\infty\left[\frac{c}{(cx+1)\ln 2}\frac{\bar{\gamma}_i}{(\bar{\gamma}_i+\bar{\gamma}x)^2}\right.\\&\left.-\log_2(cx+1)\,\frac{2\bar{\gamma}_i\bar{\gamma}}{(\bar{\gamma}_i+\bar{\gamma}x)^3}\right]\bar{\gamma}_i e^{-\frac{x}{\bar{\gamma}_i}}\,dx\\&=\int_0^\infty\frac{c}{(cx+1)\ln 2}\frac{\bar{\gamma}_i^2}{(\bar{\gamma}_i+\bar{\gamma}x)^2}e^{-\frac{x}{\bar{\gamma}_i}}\,dx\\&-\int_0^\infty\log_2(cx+1)\,\frac{2\bar{\gamma}_i^2\bar{\gamma}}{(\bar{\gamma}_i+\bar{\gamma}x)^3}e^{-\frac{x}{\bar{\gamma}_i}}\,dx.\end{aligned} \tag{22}$$

Substituting the previous expression in (21), the second term on the right hand side cancels. Therefore, we get

$$\begin{aligned}\eta_{\text{ave},3}&=\int_0^\infty\frac{c}{(cx+1)\ln 2}\frac{\bar{\gamma}_i^2}{(\bar{\gamma}_i+\bar{\gamma}x)^2}e^{-\frac{x}{\bar{\gamma}_i}}\,dx\\&=\frac{c\bar{\gamma}_i}{\bar{\gamma}(\bar{\gamma}-c\bar{\gamma}_i)^2\ln 2}\left[(\bar{\gamma}-c\bar{\gamma}_i+c\bar{\gamma}\bar{\gamma}_i)e^{\frac{1}{\bar{\gamma}}}\,\text{Ei}\left(-\frac{1}{\bar{\gamma}}\right)\right.\\&\left.+\,\bar{\gamma}\left(\bar{\gamma}-c\bar{\gamma}_i-c\bar{\gamma}_i e^{\frac{1}{c\bar{\gamma}_i}}\,\text{Ei}\left(-\frac{1}{c\bar{\gamma}_i}\right)\right)\right].\end{aligned} \tag{23}$$

When $\bar{\gamma}_j\neq\bar{\gamma}_k$, it is possible to show that

$$\begin{aligned}\eta_{\text{ave},3}&=\frac{1}{\bar{\gamma}_i(\bar{\gamma}_j-\bar{\gamma}_k)}\left[\int_0^\infty\log_2(cx+1)\right.\\&\times\left(\frac{1}{\frac{x}{\bar{\gamma}_i}+\frac{1}{\bar{\gamma}_j}}+\frac{1}{\left(\frac{x}{\bar{\gamma}_i}+\frac{1}{\bar{\gamma}_j}\right)^2}\right)e^{-\frac{x}{\bar{\gamma}_i}}\,dx\\&\left.-\int_0^\infty\log_2(cx+1)\left(\frac{1}{\frac{x}{\bar{\gamma}_i}+\frac{1}{\bar{\gamma}_k}}+\frac{1}{\left(\frac{x}{\bar{\gamma}_i}+\frac{1}{\bar{\gamma}_k}\right)^2}\right)e^{-\frac{x}{\bar{\gamma}_i}}\,dx\right],\end{aligned} \tag{24}$$

where both terms have similar form as (21). Then, using a similar integration approach for the first and second terms, the case of $\bar{\gamma}_j\neq\bar{\gamma}_k$ in (13) can be also obtained.

REFERENCES

[1] M. Ding and H. Luo, *Multi-point cooperative communication systems: Theory and applications*, Springer, 2013.

[2] Q. Cui, H. Wang, P. Hu, *et al.*, "Evolution of limited-feedback CoMP systems from 4G to 5G: CoMP features and limited-feedback approaches," *IEEE Veh. Tech. Mag.*, vol. 9, No. 3, pp. 94-103, Sept. 2014.

[3] D. Cheikh, J. Kelif, M. Coupechoux, *et al.*, "Analytical joint processing multi-point cooperation performance in Rayleigh fading," *IEEE Wireless Commun. Lett.*, vol. 1, No. 4, pp. 272-275, Aug. 2012.

[4] V. Garcia, Y. Zhou, and J. Shi, "Coordinated multipoint transmission in dense cellular networks with user-centric adaptive clustering," *IEEE Trans. Wireless Commun.*, vol. 13, No. 8, pp. 4297-4308, Aug. 2014.

[5] H. Lee, S. Kim, and S. Lee, "Combinatorial orthogonal beamforming for joint processing and transmission," *IEEE Trans. Wireless Commun.*, vol. 62, No. 2, pp. 625-637, Feb. 2014.

[6] D. Jaramillo-Ramírez, M. Kountouris, and E. Hardouin "Coordinated multi-point transmission with imperfect CSI and other-cell interference," *IEEE Trans. Wireless Commun.*, vol. 14, No. 4, pp. 1882-1896, Apr. 2015.

[7] H. Wang, X. Tao, and P. Zhang, "Adaptive modulation for dynamic point selection/dynamic point blanking," *IEEE Commun. Lett.*, vol. 19, No. 3, pp. 343-346, Mar. 2015.

[8] M. Ding, J. Zhou, Z. Yang, *et al.*, "Sequential and incremental precoder design for joint transmission network MIMO systems with imperfect backhaul," *IEEE Trans. Veh. Tech.*, vol. 61, No. 6, pp. 2490-2503, Jul. 2012.

[9] 3GPP. R1-122895, "Way forward on the maximum size of CoMP measurement set," TSG RAN WG1, 2012.

[10] S. T. Chung and A. J. Goldsmith, "Degrees of freedom in adaptive modulation: A unified view," *IEEE Trans. Commun.*, vol. 49, No. 9, pp. 1561–1571, Sept. 2001.

[11] S. Ye, R.S. Blum, and L.J. Cimini Jr, "Adaptive OFDM systems with imperfect channel state information," *IEEE Trans. Wireless Commun.*, vol. 5, No. 11, pp. 3255-3265, Nov. 2006.

[12] M. S. Alouini and A. J. Goldsmith, "Adaptive modulation over Nakagami fading channels," *Wireless Personal Commun.*, vol. 13, No. 1, pp. 119-143, May 2000.

[13] J. Proakis, M. Salehi, *Digital Communications*, 5th edition, New York, NY, USA: McGraw-Hill Education, 2007.